ISSN: 2710-0588 DOI: 10.29556/FSE.202109_1(6).0015

Application of Tanguchi Method in Robust Design of Permanent Magnet Synchronous Motor

Xianghong He[1,*], Dalu Nie[1], Zhenguang Zhu[1], Tianxiong Lu[2]

[1]College of General Education, Guangdong University of Science and Technology, Guangdong 523808, China;

[2]Hangzhou EasiTech CO. LTD, Zhejiang, 310008, China.

*misshe@163.com

Abstract

To avoid the potential unstable factors in motor design, this paper improve the original Taguchi method and provide a more perfect robust process. With this method, the author use EasiMotor software as motor design and dynamic performance analysis platform, design a permanent magnet synchronous motor with low torque pulsation and high average torque. The results show that, the optimization design using this method can significantly reduce the torque pulsation and increase the design robustness.

Keywords

PMSM; Torque Pulsation; FEM; Taguchi Method; Robust Analysis.

1. Introduction

In the servo system, the servo accuracy is a very key system index, and the torque ripple of permanent magnet synchronous motor is the key factor affecting the servo accuracy of the servo system. However, in the actual production process of permanent magnet synchronous motor, the deviation of motor material, installation size, magnetic steel characteristics and other factors will greatly affect the pulsating torque value of the motor. Therefore, how to reasonably select the interval of design variables from the perspective of design, fully consider the deviation influence of installation, materials and magnetic steel, so as to improve the robustness and anti-interference ability of products and meet the servo performance of servo system has become an important research topic.

Among the many robust methods, Taguchi [1] is favored for its low cost and high efficiency. Taguchi method uses orthogonal tables to arrange experiments, and uses signal-to-noise ratio to measure stability. With a few experiments, the best solution with good performance and insensitivity to noise can be obtained. At the same time, simple addition and subtraction operations can be added to evaluate the parameters of each parameter or influence level. Because of its ease of combining virtual experiments, Taguchi method combined with finite element for motor design has become a new type for engineer in the early stage of product development [2,3].

However, in the robust design, only controllable factors were considered [4,5], and the noise factors inevitably generated during the manufacturing and processing of the motor were not considered. At the same time, there was very little or no evaluation of the "best solution" obtained. To be sure, these potential hazards can easily cause unstable product quality during mass production. In view of this, this paper designs and optimizes a surface-mount permanent magnet synchronous motor based on the more complete Taguchi method's robust design process, while considering the control factors that affect torque ripple and the noise factors in the processing process. Judging from the simulation results, the motor designed by the optimal

ISSN: 2710-0588 DOI: 10.29556/FSE.202109_1(6).0015

scheme is greatly improved in terms of performance and stability compared with the original design.

2. Robust analysis of Taguchi method

Figure 1 is a schematic diagram of the improved Taguchi method's robust design process. This article will follow this process to an 8-pole 24-slot surface-mount permanent magnet synchronous motor with a rated power of 500W and a rated speed of 1500RPM with low torque ripple, High average torque is the goal to optimize the motor structure.

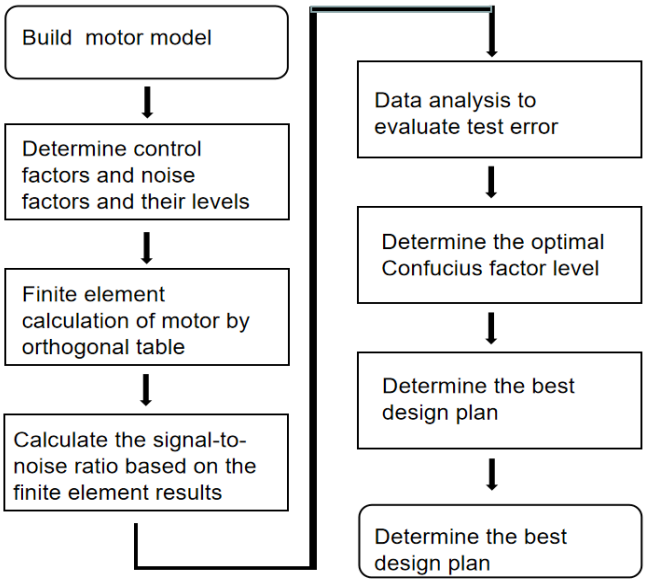

Figure 1. Improved Taguchi Robust Design Process

The motor structure and controllable factor parameter diagram are shown in Figure 2. The controllable factors and noise factors and their levels are shown in Table 1 and Table 2. The original design scheme is the bold part of Table 1, namely A2B2C2D2E2. The selection of the control factor level is mainly based on the expected improvement direction of the torque ripple and the allowable range of design variables, while the noise factor level is mainly calculated by the motor processing technology and dimensional chain.

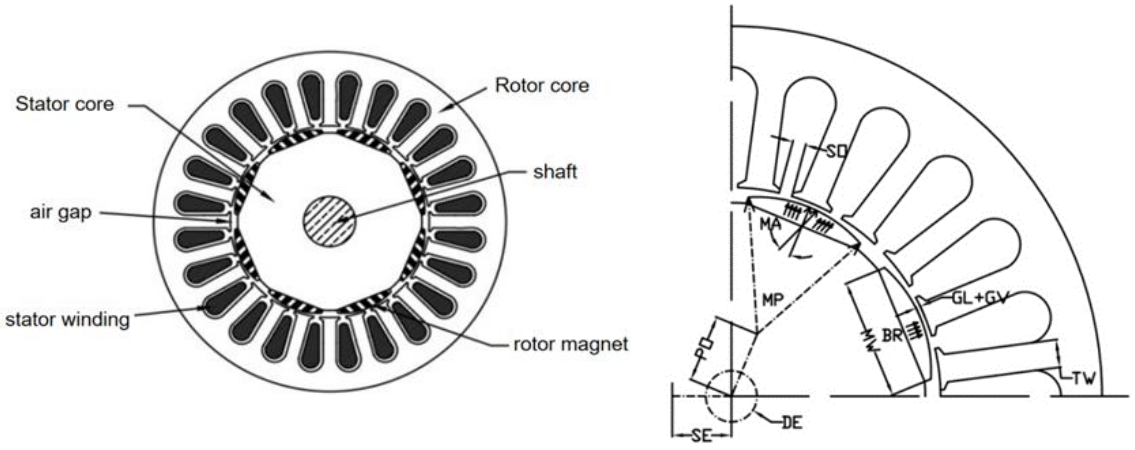

Figure 2. Permanent magnet synchronous motor structure diagram and controllable factor parameter diagram

ISSN: 2710-0588 DOI: 10.29556/FSE.202109_1(6).0015

Table 1. Control factors and their levels

Control factor	Level 1	Level 2	Level 3
Polar arc offset PO (mm)	A1(8.7)	A2(9.2)	A3(9.7)
Corresponding pole arc coefficient PO	B1(0.76)	B2(0.78)	B3(0.8)
Slot Opening SO (mm)	C1(1.60	C2(1.8)	C3(2)
Tooth width TW (mm)	D1(3.60	D2(3.8)	D3(4)
Air gap length GL (mm)	E1(0.5)	E2(0.6)	E3(0.7)

Table 2. Noise factors and their levels

Noise factor	Level 1	Level 2
Magnet position offset MP (mm)	0	0.2
Remanence error BR (Tesla)	1.01	1.04
Magnetization angle error MA (degree)	0	1
Air gap height error GV (mm)	-0.03	0.03
Sensor position deviation angle SP (degrees)	0	0.1
Static eccentricity SE (mm)	0	0.05
Dynamic eccentricity DE (mm)	0	0.05

Because the experimental factors include both control factors and noise factors, the experimental factor configuration orthogonal table selects the combination of internal and external orthogonal tables, as shown in Table 3. Columns 2-6 are the control factor configuration tables, and the standard orthogonal table is selected. Columns 2-7th in the table selection L_{18} $(2^1 \times 3^7)$ and columns k_1-k_8 are the configuration table of the noise factor, and the standard orthogonal table $L_8(2^7)$ is selected.

For each group of tests (18 groups in this experiment) determined by Taguchi method orthogonal table, according to the configuration of noise factors, the electromagnetic field model of the corresponding motor is established by using the finite element method on Easimotor software, and the corresponding field results and output torque curve are obtained (Fig. 3).

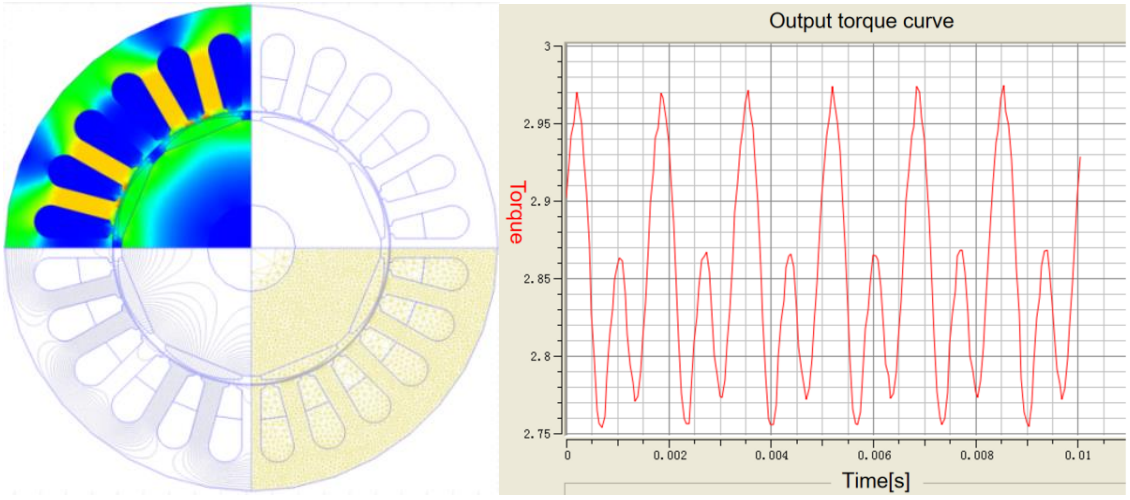

Figure 3. (Left) Motor geometry model, finite element mesh, magnetic field lines and field calculation results (Right) Output torque curve

Use the formula for the output torque curve

$$K_{\mathrm{mb}} = \frac{T_{max} - T_{min}}{2T_{\mathrm{avg}}} \quad (1)$$

Obtain the torque ripple value of each control combination under the corresponding noise, that is, column $(K_1 - K_8)$ in Table 3. Among them, T_{max}, T_{min}, T_{avg}, are the maximum, minimum and average values of torque in a cycle.

ISSN: 2710-0588 DOI: 10.29556/FSE.202109_1(6).0015

The motor design requires that the torque ripple is as small as possible, so the corresponding calculation formula for small signal noise is:

$$S_N = -10\, log_{10}\left(\frac{1}{10}\sum_{i=0}^{n} k_i^2\right) \quad (2)$$

Among them, S/N_all is the signal-to-noise ratio of each group of experiments (here there are 18 in total), and n is the number of experiments performed in a group of experiments (in this case, n=8). The obtained torque ripple and the corresponding signal-to-noise ratio are shown in Table 3. In this way, after 18×8=144 simulation experiments, accurate results can be obtained, which is far less than the number of full factor experiments (729×128).

Table 3. Torque ripple experimental values and corresponding signal-to-noise ratio SN

L18							L8								S/N_all	Kmean
	1	2	3	4	5	6	MP/BR/MA/GV/SP/SE/DE									
	PO	MW	SO	TW	GL	E	k_1 1111111	k_2 1112222	k_3 1221122	k_4 1222211	k_5 2121212	k_6 2122121	k_7 2211221	k_8 2212112	S/N_all	k_mean
1	A1	B1	C1	D1	E1	F1	0.1001	0.087043	0.09481	0.08615	0.09238	0.0896	0.09057	0.07901	20.9	0.08996
2	A1	B2	C2	D2	E2	F2	0.0839	0.067984	0.07694	0.07136	0.07501	0.0683	0.07093	0.06721	22.746	0.0727
3	A1	B3	C3	D3	E3	F3	0.0631	0.051595	0.05749	0.05568	0.05729	0.0522	0.05219	0.05106	25.16	0.05507
4	A2	B1	C1	D2	E2	F3	0.0783	0.06364	0.07845	0.06626	0.06861	0.0643	0.07025	0.06244	23.187	0.06903
5	A2	B2	C2	D3	E3	F1	0.0559	0.047542	0.05381	0.05244	0.05381	0.0499	0.05265	0.04868	25.695	0.05184
6	A2	B3	C3	D1	E1	F2	0.1315	0.079109	0.08777	0.08746	0.08098	0.0814	0.083	0.07058	20.971	0.08773
7	A3	B1	C2	D1	E3	F2	0.0829	0.072663	0.07651	0.07757	0.08214	0.0757	0.0788	0.07687	22.164	0.07789
8	A3	B2	C3	D2	E1	F3	0.125	0.077053	0.084	0.07695	0.07457	0.0759	0.08117	0.0674	21.472	0.08276
9	A3	B3	C1	D3	E2	F1	0.0548	0.041809	0.04778	0.04283	0.04671	0.0423	0.04513	0.04144	26.83	0.04535
10	A1	B1	C3	D3	E2	F2	0.0942	0.074338	0.08187	0.07917	0.08057	0.074	0.07753	0.07343	21.978	0.07938
11	A1	B2	C1	D1	E3	F3	0.0662	0.054859	0.0633	0.05943	0.06202	0.0554	0.06192	0.05404	24.466	0.05966
12	A1	B3	C2	D2	E1	F1	0.0751	0.069638	0.07756	0.07266	0.07017	0.0721	0.07201	0.06098	22.924	0.07127
13	A2	B1	C2	D3	E1	F3	0.0746	0.073799	0.07991	0.07605	0.07227	0.0765	0.0756	0.06488	22.579	0.0742
14	A2	B2	C3	D1	E2	F1	0.0827	0.076492	0.08634	0.07873	0.0863	0.0773	0.0849	0.07683	21.798	0.0812
15	A2	B3	C1	D2	E3	F2	0.051	0.038658	0.04447	0.04413	0.04522	0.0403	0.04418	0.0389	27.226	0.04335
16	A3	B1	C3	D2	E3	F1	0.0799	0.073966	0.07688	0.07766	0.08277	0.0762	0.07917	0.07824	22.143	0.0781
17	A3	B2	C1	D3	E1	F2	0.0573	0.057261	0.0615	0.05426	0.05455	0.0576	0.06107	0.04973	24.916	0.05667
18	A3	B3	C2	D1	E2	F3	0.0637	0.058903	0.06804	0.06265	0.06776	0.0599	0.06429	0.05942	23.99	0.06308
													average value		23.4	0.0688

According to the experimental data in Table 3, the factor analysis table and the corresponding analysis chart of the control factor signal-to-noise ratio are obtained by means of analysis.

Table 4. SNR and its ranking under each level of controllable factors

Level	Pole a arc offset PO	B-pole arc coefficient MW	C slot opening width SO	D tooth width TW	E air gap length GL	F other errors
1	23.029	22.159	**24.588**	22.381	22.294	23.382
2	23.576	23.515	23.35	23.283	23.421	23.334
3	**23.586**	**24.517**	22.254	**24.526**	**24.476**	23.476
Range Rj	0.557	2.358	2.334	2.145	2.182	0.048
Ranking	5	1	2	4	3	

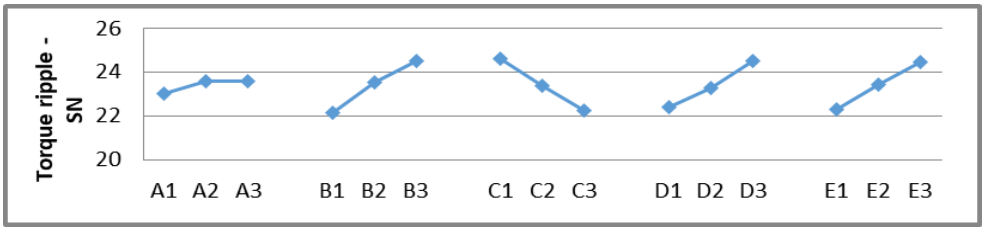

Figure 4. SN factor analysis under various levels of controllable factors

ISSN: 2710-0588 DOI: 10.29556/FSE.202109_1(6).0015

Because the larger the signal-to-noise ratio, the more stable the performance is. The maximum level of controllable factors is selected (the black body in Table 4, the highest point in Figure 4). The optimization scheme is A3 B3 C1 D3 E3, that is, the parameter combination: the polar arc offset is 9.7mm, The design is optimal when the pole arc coefficient is 0.8, the slot opening width is 1.6mm, the tooth width is 4mm, and the air gap length is 0.7mm.

According to the range ranking and the Taguchi method half of the original [7], it can be seen that the pole arc coefficient B, the slot opening width C and the air gap length E are the control factors that have a significant impact on the torque ripple. This is consistent with the results of the SNR analysis of variance (limited to space, not repeated here). However, compared with the complex statistical work that needs to be carried out in the variance experiment, Taguchi method only needs to perform simple addition and subtraction and simple sorting operations to obtain the desired results, so its execution and efficiency have significant advantages.

At the same time, the factor analysis table and factor analysis diagram of the noise factor to the torque ripple signal-to-noise ratio are shown in Table 5 and Figure 5. The average value analysis shows that within the design space, the air gap height error GV and the static eccentric SE are counter-rotating. The influence of moment pulsation is obvious. The magnetization angle deviation has little effect. Knowing the influence of noise factors on quality characteristics can play an effective guiding role in the actual processing process.

Table 5. Signal-to-noise ratio SN and ranking under each level of noise factor

S/N and its ranking under each level of noise factor							
Level	Magnetic steel position offset MP	Remanence error BR	Magnetization angle error MA	Air gap height error GV	Sensor position deviation angle SP	Static eccentricity SE	Dynamic eccentricity DE
1	28.5153	28.6306	28.57	28.2541	28.6528	28.4369	28.5258
2	28.639	28.5238	28.5844	28.9	28.5016	28.7175	28.6285
Range Rj	0.1237	0.1068	0.0144	0.6459	0.1512	0.2806	0.1027
Ranking	4	5	6	1	3	2	7

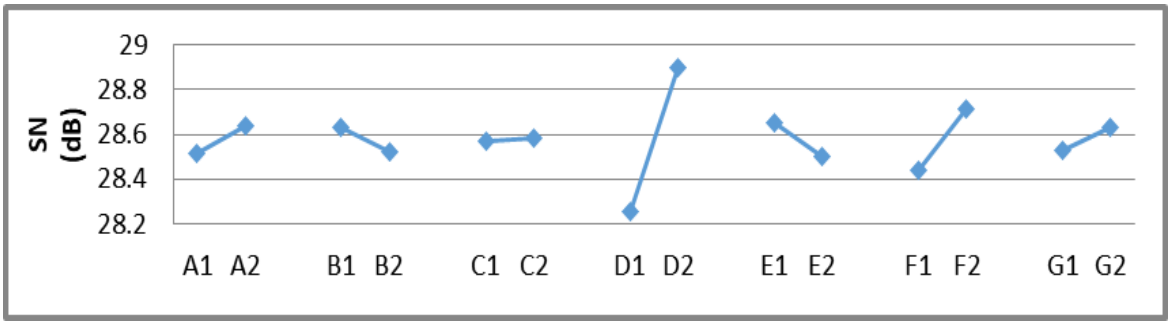

Figure 5. Noise factor response analysis diagram

In order to avoid potential hazards in the design that cause product quality instability in mass production, this article adds a confirmation experiment on the optimization scheme, and a new definition of effective samples:

$$m_e=\frac{\text{Total number of experimental data}}{\text{the total degrees of freedom in the predictive formula}}=\frac{18}{9}=2$$

This way, with a confidence level of 99%:

The confidence interval of the predicted value of the torque ripple signal-to-noise ratio is: 0.86724.

The confidence interval of the torque ripple signal-to-noise ratio confirmation value is 1.502097.

ISSN: 2710-0588 DOI: 10.29556/FSE.202109_1(6).0015

Since the original scheme (A2 B2 C2 D2 E2) and the optimized scheme (A3 B3 C1 D3 E3) are not in the orthogonal table, additional experiments are required. The specific values and the corresponding confidence intervals obtained are shown in Table 6 and Table 7.

Table 6. Predicted and experimental values of original design and optimized design quality characteristics (torque ripple)

Design	Predicted S/N	torsion arterial motion prediction value	Experimental calculation SN	Experimental calculation torque pulsation
Original design	23.492	0.066206	23.8536	0.06416799
Optimal design	26.787	0.045006	28.5223	0.037487478

Table 7. Confidence interval of original design and optimized design

Confidence interval	Original design	Original design confidence interval		Optimal design	Optimal design confidence interval	
0.86724	23.492	22.62476	24.35924	26.787	25.91976	27.65424
1.502097	23.8536	22.3515	25.3557	28.5223	27.0202	30.0244

It can be seen from Table 7 that the prediction intervals of the original plan and the optimized plan overlap with the experimental value interval. From this, it can be determined that the predicted values of the optimized plan and the original plan are close enough to the experimental calculated values to determine the optimized plan (A3 B3 C1 D3 E3) accuracy and credibility.

3. Scheme comparison

Table 8 shows the torque ripple signal-to-noise ratio, torque ripple value, and average torque value of the original design and the optimized design. It is obvious that the optimized torque ripple is greatly reduced, from 0.0642 to 0.0375, which reduces 0.0267, an increase of nearly 41.6%, and the average torque has not only increased numerically, the deviation percentage has also decreased from the original 6.74% to the current 5%. It can also be clearly seen from the output torque curve comparison chart in Figure 6 that the peak value of the optimized torque curve is significantly reduced. Therefore, from the perspective of quality characteristics, the optimized design does greatly reduce the torque ripple and increase the average value.

Table 8. The ratio of original design and optimized design signal-to-noise ratio, torque ripple and average torque

Design	Predicted S/N	calculated torque ripple	Average torque	deviation degree
Original design	23.8536	0.0642	2.848835	6.74%
Optimal design	28.5223	0.0375	2.857612	5%
Improvement rate	19.57%	41.6%	3.1%	

Figure 6 is the peak-to-peak dispersion diagram of the average torque and torque ripple after a given noise under the three different design schemes of the optimized scheme, the original scheme and the scheme 1. It can be clearly seen from the figure that the optimized scheme (red square) Whether in the longitudinal direction or torque ripple, or in the transverse direction, the average torque, the dispersion is more concentrated than the original design and scheme 1, which shows that the optimized design is far superior to the original design in terms of stability. In summary, through Taguchi method, the optimized parameter combination scheme is A3 B3 C1 D3 E3 with a small number of experiments (Taguchi method 144 times, full factor 5452 times). At the same time, using the half principle, it is known that within the design space, the

ISSN: 2710-0588 DOI: 10.29556/FSE.202109_1(6).0015

pole arc coefficient, slot opening width and air gap length are the control factors that have a significant impact on the torque ripple. The air gap height error and static eccentricity are the control factors for the torque. The pulsation affects the obvious noise factor, and the simulation results also show that the optimized scheme is greatly improved compared with the original design in terms of quality and stability. The final definitive experiment guarantees the accuracy and credibility of the data in all the experimental schemes.

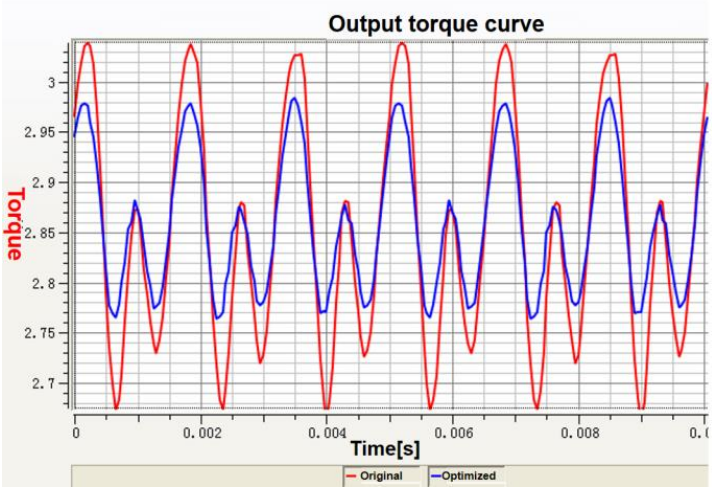

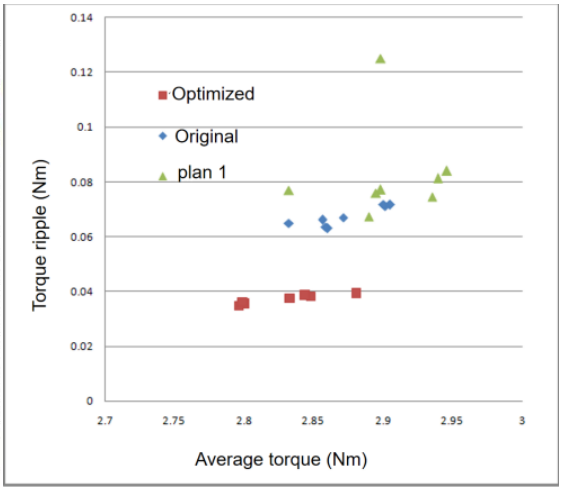

Figure 6. Comparison of torque curves (original, optimized) Figure 7 Stability distribution of scheme

4. Summary

In summary, using the Optimal Taguchi method combined with finite element for robust motor design has the following advantages:

1). The internal and external orthogonal table design covers the distribution level of the factors (including control factors and noise factors), which can effectively reduce the number of experiments, and has significant advantages in execution and efficiency. (For example, Taguchi method only needs 144 times, while full factors require 5452 times).

2). The signal-to-noise ratio is used as a measure of robustness, which meets the multi-objective optimization requirements for motor performance and dispersion interval.

3). Use simple addition and subtraction to quickly and easily find out the important influencing factors (control factor and noise factor) that affect the specific performance of the motor.

4). The optimized scheme obtained by Taguchi method has better performance quality and smaller performance dispersion interval.

5). Confirm the experiment to ensure the accuracy and credibility of the optimization plan data.

As robustness analysis has become more and more a hot topic in the research and development of high-performance motors, the transition from a single robust design method to multiple robust design methods and the combination of intelligent optimization methods has gradually become a development direction. Therefore, the transition from a single goal to multi-objective optimization will become a development direction. The author's next research goal.

Acknowledgments

This paper was financially supported by the Natural Science General Project of Guangdong University of Science and Technology: Application of Taguchi Method in Robust Optimal Design of Motors (GKY-2019KYYB-26):

ISSN: 2710-0588 DOI: 10.29556/FSE.202109_1(6).0015

References

[1] Taguchi Genichi, Introduction to Taguchi Quality Engineering, published by China Productivity Center.

[2] Xia Jiakuan, Yu Bing, Huang Wei. Optimal design of permanent magnet motor structure to reduce cogging torque [J], Electrical Technology, 2009, 12(): 23-25.

[3] Lv Liyang, using genetic algorithm and Taguchi method to optimize the design of surface type permanent magnet synchronous motor [D], Master's thesis of Fengjia University. 2008.

[4] S.X.Chen,T.S.Low,and Bruhl,The robust design approach for reducing motor on cogging torque in permnenet magenet motors [J], IEEE Trans,Magn, 1998, 34(4): 2135-2137.

[5] R.K.Roy, Design of Experiments Using the Tanguchi Approach. New York: Wiley, 2001.

[6] Huang Yong, Research on the Key Processing Technology of AC Permanent Magnet Servo Motor [J], Mechanical Design and Manufacturing, 2002, 5: 105-125.

[7] Lin Xiuxiong, Actual Combat Techniques of Taguchi Method, Shenzhen: Haitian Press, 2008.